A method for the determination of local packing factor distribution of a packed pebble bed by the improved line-based averaging method

Baoping Gong [*], Hao Cheng, Juemin Yan, Long Zhang

Southwestern Institute of Physics, Chengdu 610041, China

ARTICLE INFO

ABSTRACT

The packing factor is an important parameter for describing the internal structural features in pebble beds, which have a significant influence on the heat and mass transfer behavior and the thermo-mechanical properties of the pebble bed. A comprehensive understanding of the packing structure is essential for the design and optimization of the pebble bed and can promote the application of the pebble bed. In this work, an improved line-based averaging method was proposed to calculate the local packing factor or local porosity distribution and validated by comparing the results with those obtained from experimental and numerical studies of cylindrical packed pebble bed. Furthermore, the local packing factor distributions in the angular-radial plane of the cylindrical pebble bed were revealed for the first time. In addition, the line-based averaging method has been applied to reveal the local packing factor distributions in the annular pebble beds, U-shaped pebble beds and hexagonal pebble beds. The main feature of this method is the ability to calculate and plot contour maps of local packing factor or porosity distributions for columnar pebble beds of arbitrary shapes, especially the local packing factor distributions in the cross-sectional plane and the angular-radial plane.

1. Introduction

The packing characteristics of a packed pebble bed have a significant impact on the heat transfer performance, fluid flow characteristics, and thermo-mechanical properties of the pebble bed [1-6]. For example, in a fusion reactor blanket pebble bed, the packing structures of tritium breeder pebbles and neutron multiplier pebbles are closely related to the effective thermal conductivity of the breeder pebble bed [7-9], the purge gas flow characteristics through the pebble bed [10-12], the tritium breeder performance of the blanket [13], and the thermal-mechanical properties of pebble beds [14]. In a high-temperature gas-cooled reactor, the fuel pebble packing structures in the reactor core will affect the heat transfer performance and thermal conductivity of the nuclear fuel pebble bed [15,16]. Therefore, a comprehensive understanding of the pebble packing structure is essential for the design optimization of nuclear reactors.

The packing factor, or called packing fraction and packing density, is an important parameter for describing the structural features of pebble beds. The macroscope packing properties of the packed bed, such as the average packing factor and average porosity, can be obtained through physical packing experiments. To obtain the radial and axial packing

factor distribution of pebble beds nondestructively in experiments, some non-destructive testing technology are required, such as, X-ray CT technology [17], MRI detection techniques [18] and γ ray transmission technique [19]. These non-destructive testing technologies are costly and require expensive equipment. However, numerical simulation based on the discrete element method (DEM) enables the direct acquisition of pebble center coordinates and radius [20], which can be utilized in subsequent calculations to derive the average packing factor (porosity), radial/axial porosity (packing factor) distribution, etc. of the pebble bed. Consequently, the accurate and expeditious calculation of the packing factor and porosity of the pebble-packed bed, based on the data of pebble center coordinates and radius, is of paramount importance for the analysis of the packing structure of the pebble bed.

Once the pebble center coordinates and pebble radii have been obtained, the average packing factor and radial/axial packing factor of a pebble bed can be calculated using volume-based averaging method [21, 22], area-based averaging method [23], and line (arc-length) averaging methods [24-26], respectively. The volume averaging method is usually employed to calculate the average packing factor (also known as porosity) of a pebble bed, with the primary objective of determining the total volume of pebbles present within a specified region. In the case of

gravimetric methods employed in packing experiments, the total volume of pebbles is calculated primarily based on their weight and density. Furthermore, the measuring circle/sphere method, which is also a volume averaging method, was employed to ascertain the average packing factor of the pebble bed [27]. In volume average methods, the volume of the portion of the pebble that intersects the computational boundary and is within the computational region is usually computed accurately to improve the accuracy of the computation. In addition, Mueller proposed a volume-based method by dividing the pebble bed into a large number of radial annular layers to calculate the radial porosity in cylinder pebble bed [21]. The radial packing factor is expressed in terms of the solid volume segments. By reducing the thickness of the radial annular layer, an area-averaging method was proposed by replacing the radial annular layer with a radial cylindrical surface [24] to calculate radial packing factor. However, in this method, more complicated surface integration is requirements for cylindrical pebble beds because the intersection of pebbles and cylindrical surfaces is an elliptical surface [28]. To simplify the calculation of surface integration, Mueller proposed an arc-length based averaging method [24]. The intersecting surfaces of pebbles with cylindrical cutting surfaces are divided as arcuate microelements in the axial direction. The local packing factor at the position (r, z) is obtained by calculating the ratio of the sum of the intersecting arc lengths to the circumference of the cross-section circle. Bester [25] proposed a vertical-line based averaging method to calculate the angular and radial packing factor of cylindrical pebble beds. However, the area-based averaging method and the arc-lengths-based averaging method are all limited to the calculation of the radial packing factor for cylindrical beds and not applicable for complex shaped pebble beds, such as, polygonal pebble beds, U-shaped pebble beds, elliptical columns, and other special shaped pebble beds.

Therefore, in our previous work, a line-based averaging method was proposed to calculation the local packing factor distribution in rectangular pebble beds [26]. In this study, an extend of the line-based

averaging method were reported to calculate the local packing factor distribution for arbitrarily shaped column beds with spherical particles. The local packing factor is calculated by determining the length of the line segment where the particle intersects with a straight line. The detailed line-based averaging method is described in Section 2. This method can be generalized to the calculation of axial and radial packing factors, see Section 3. The validation and the application of the line-based averaging method are presented in Section 4 and Section 5, respectively. Finally, some conclusions will be summarized in Section 6.

2. Line-based averaging method

To reveal the local packing characteristics in pebble bed, the local packing factor is introduced in this study based on the line-averaged method. This method is mainly based on drawing an orthogonal grid in the plane perpendicular to the axial direction and calculating the line-averaging local packing factor at each grid point. Then, the axial/radial packing factor distribution of the pebble bed can be obtained by calculating the average according to the axial/radial position. The total average packing factor can be calculated by averaging over the whole areas. The flowchart of the local packing factor calculation based on the line-averaging method is shown in Fig. 1.

Firstly, coordinate data of the pebble bed, such as the center coordinate and radius of the pebbles, are obtained. These pebble data can come from discrete element method simulations or from CT scanning experiments. Secondly, the parameters and boundary conditions must be set, including the computational region boundary, the packing factor distribution plane, and the orthogonal grid size. Thirdly, an orthogonal grid is drawn in the distribution plane according to the grid size settings and grid point coordinates are obtained. Subsequently, the line-averaged local packing factor is calculated for each grid point through an iterative process. If the local packing factors are calculated for all grid points, proceed to the next step to begin plotting the local packing factor
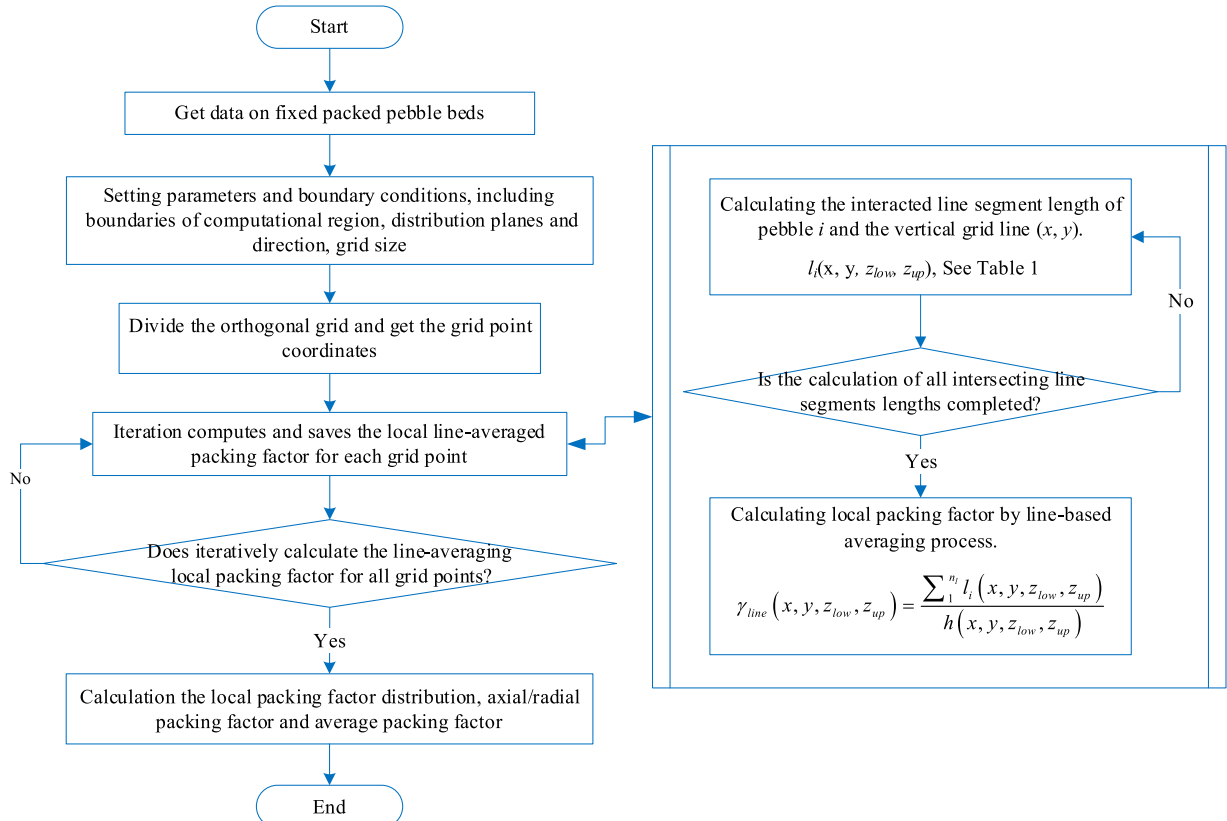

Fig. 1. Flowchart of local packing factor calculation based on line averaged method.

planar distribution of the pebble bed and calculating the axial and radial packing factor distributions and the average packing factor of the pebble bed.

For instance, for the rectangular and cylindrical pebble bed, the pebble bed region can be meshed firstly in the cross-sectional plane such as the x-y plane, as shown in Fig. 2. The grid size can be manually set according to needs. The red point is the grid point of (x, y). In addition, there are five types of interactions between pebbles and upper/lower boundary, as shown in Fig. 3(a). Sections of a boundary pebble above the upper boundary and below the lower boundary have to be excluded.

Then, the local packing factor, $\gamma_{line}(x, y, z_{low}, z_{up})$, at each grid point (vertical grid line at grid point) can be calculated by the ratio of the sum of these interacted line segment lengths to the vertical line segment length, as shown in Fig. 3b. The line-averaged local packing factor $\gamma_{line}(x, y, z_{low}, z_{up})$ can be expressed as following:

$$\gamma_{line}\left(x, y, z_{low}, z_{up}\right) = \frac{\sum_1^{n_l} l_i\left(x, y, z_{low}, z_{up}\right)}{h\left(x, y, z_{low}, z_{up}\right)}, \tag{1}$$

where, h (x, y, z_{low}, z_{up}) is the vertical line segment length and determined by $|z_{low}-z_{up}|$. n_l is the number of pebbles intersecting with the vertical line. $l_i(x, y, z_{low}, z_{up})$ is the interacted line segment length of pebble i and the vertical grid line.

It is assumption that the pebbles are hard spheres or particles. The slight overlap between pebbles is so small that it can be ignored. Thus, accord to the relation of pebbles and the vertical grid line and upper/lower boundary, their interaction can be divided into five ways as displaced in Table 1. In addition, the calculation formula of the intersecting line segments length, l_i (x, y, z_{low}, z_{up}) also displayed in Table 1. After obtaining l_i (x, y, z_{low}, z_{up}), the local packing factor of the grid point can be calculated by Eq. (1). After obtaining the local packing factor for each grid point, the local packing factor distribution can be also obtained.

3. Calculation of packing factors

Both the axial packing factor and radial packing factor can reflect the wall effect on the pebble packings close to the container walls. After obtaining the local packing factor for each grid point (line), the radial and axial packing factor distribution can also be obtained by further processing.

3.1. Radial packing factor

For the pebble packing in cylindrical and annular containers, radial packing factor is recommended to describe the pebble packing structures which can be also obtained by the line-based averaging method. Along the radial direction, the pebble bed is cut by many concentric

cylindrical surfaces with specified radial position steps. The radical cylindrical cutting surface can be discretized as numerous vertical lines along the circumferential direction with specified steps., as shown in Fig. 4. After obtaining the local packing factor at each vertical line, the radial packing factor, $\gamma_{line}(R_{radial})$, of a cylindrical pebble bed can be obtained by averaging the local packing factor along the circumferential direction.

$$\gamma_{radial}\left(R_{radial}, z_{low}, z_{up}\right) = \frac{\sum_1^{n_{circum}} \gamma_{line}\left(x, y, z_{low}, z_{up}\right)}{n_{circum}} \tag{2}$$

where, $R_{radial} = \sqrt{(x - x_o)^2 + (y - y_o)^2}$, x_o and y_o are the Coordinates of the central axis of the cylinder pebble bed. z_{low} and z_{up} are the low and up limitation along the vertical direction. n_{circum} is the number of the divided vertical lines in cylindrical surfaces.

The line-based averaging local packing factor $\gamma_{line}(x, y, z_{low}, z_{up})$ can be expressed as following:

$$\gamma_{line}\left(x, y, z_{low}, z_{up}\right) = \frac{\sum_1^{n_l} l_i\left(x, y, z_{low}, z_{up}\right)}{h\left(x, y, z_{low}, z_{up}\right)}, \tag{3}$$

where, h (x, y, z_{low}, z_{up}) is the vertical line segment length. n_l is the number of pebbles intersecting with the vertical line. $l_i(x, y, z_{low}, z_{up})$ is the interacted line segment length of pebble i and the vertical line. The calculation of $l_i(x, y, z_{low}, z_{up})$ can refer the Table 1.

3.2. Axial packing factor

For the rectangular or cubic pebble beds, Axial packing factor is always used to reveal the flat wall effect on the packing structure. The axial packing factor can be easily calculated based on both the area-based averaging method and line-based averaging method. For the pebble packing near a flat plane, such as pebble packing close to the bottom/top wall in cylindrical pebble bed, or pebble packing in cubic/rectangular container, the axial packing factor is preferred to reflect the local packing structure. As an example, Fig. 5 shows the calculation methods of axial packing factor based on both the area-based averaging method and line-based averaging method. Lots of parallel cutting planes were inserted into the pebble bed with a specific distance step. All pebbles interact with cutting planes to produce many cross-sectional circles. The axial packing factor can be determined based on area-based averaging method as:

$$\gamma_{axial}\left(L_{axial}\right) = \frac{\sum_1^{n_{cut}} S_i^{cut}}{S_{cutplane}}, \tag{4}$$

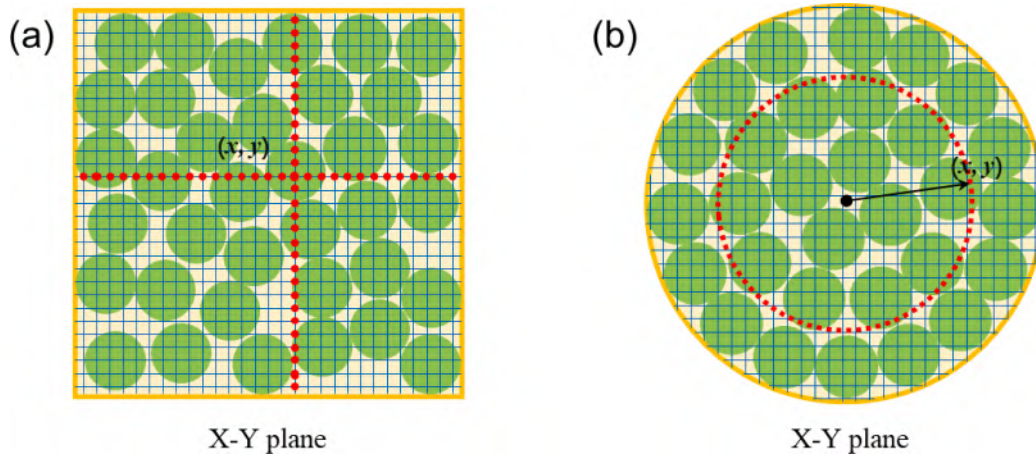where, n_{cut} is the number of pebbles interacted with cutting planes at

Fig. 2. Schematic of the orthogonal grid in cross-sectional plane in (a) rectangular and (b) cylinder pebble bed.
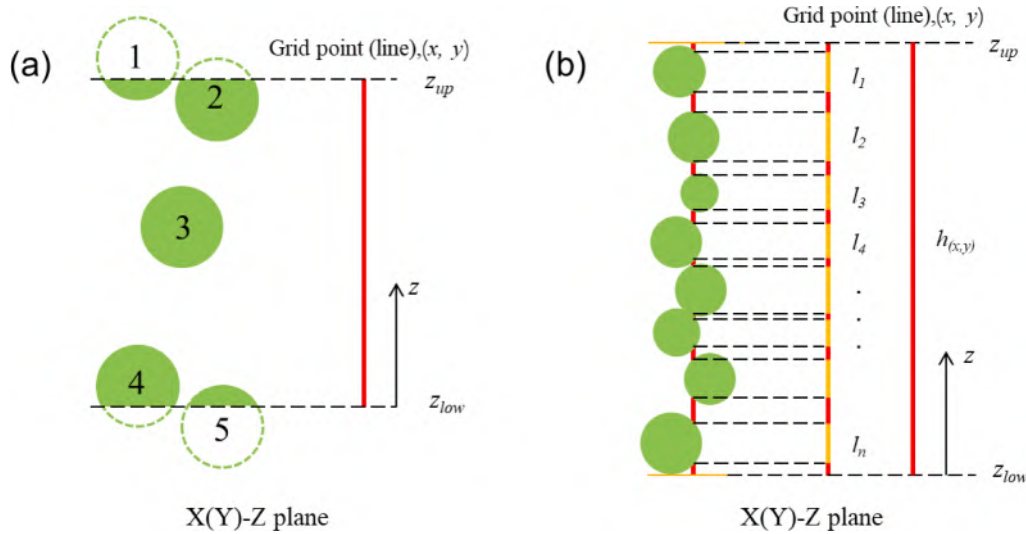
Fig. 3. Schematic of interaction (a) between pebbles and upper/lower boundary, (b) between pebbles and grid line.

position of L_{axial}. $S_{cutplane}$ is the area of the cutting plane. S_i^{cut} is the cross-sectional circle area of pebble i interacted with the cutting plane, which can be calculated by the

$$S_i = \pi r_{cut}^2 = \pi \left(r_i^2 - L_{cutp_i}^2 \right) \tag{5}$$

where r_i is the radius of pebble i, L_{cutp} is the distance between the cutting plane and the touched pebble center, $0 < L_{cutp} < r_i$.

For the line-based averaging method, the axial packing factor can be expressed as:

$$\gamma_{axial}\left(L_{axial}, z_{low}, z_{up}\right) = \frac{\sum_1^{n_{cutplane}} \gamma_{line}\left(x, y, z_{low}, z_{up}\right)}{n_{cutplane}}$$

where L_{axial} is the distance to boundary wall along the axial direction, $L_{axial} = |x-x_o|$ or $|y-y_o|$ or $|z-z_o|$, x_o or y_o or z_o are the coordinate of the one boundary wall. $n_{cutplane}$ is the number of the divided vertical lines in cutting plane.

3.3. Local packing factor distribution

The axial packing factor and radial packing factor distribution can reflect the one fixed wall effect on the adjacent pebble packing structures. However, in the corner region of the rectangular pebble bed or other irregularly shaped pebble beds, the packing structure is affected by two or more fixed wall. At this stage, the most effective means of visualizing the influence of multiwall effects is through the use of a cloud map displaying the local packing factor distribution. This approach enables the viewer to gain a clear understanding of the impact of these effects on the local packing structure of pebble bed. The cloud map of the local packing factor distribution can be drawn from the local packing factors obtained from the calculations in Section 2 by Eq. (1).

4. Validation in the cylindrical packed pebble bed

Cylindrical pebble bed is widely used in the chemical and energy fields, such as catalyst packed fixed bed [29], nuclear fuel pebble bed in the high-temperature gas-cooled reactor core [30], etc. There are a lot of data of pebble packing structures in cylindrical and rectangular packed pebble bed. Therefore, the line-based averaging method was validated in this work by comparing the results with those obtained from experimental [31,32] and numerical studies [24] of cylindrical packed pebble bed. Fig. 6 shows a cylindrical bed packed with the mono-sized spherical pebbles, which were obtained by a DEM simulation. The cylinder and
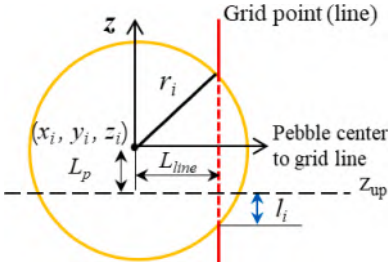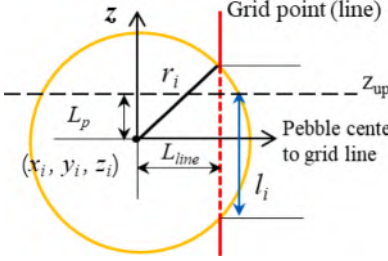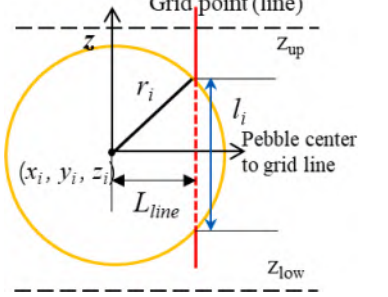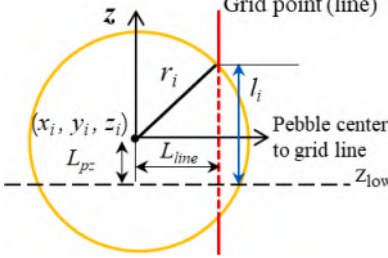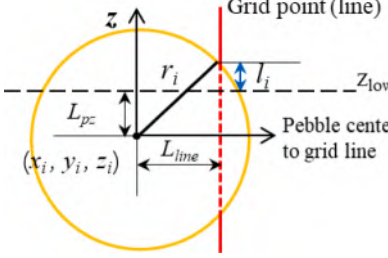
pebble diameter are 15 mm and 1 mm, respectively. In the validation, the radial and axial packing factor distributions are considered in the evaluation.

As shown in Fig. 6, an obvious wall effect on the pebble packing can be observed in the top view of the pebble bed and the pebble center distribution, where pebble centers were projected into the bottom wall. In the region proximate to the wall, the pebbles are arranged in a relatively more regular manner, resulting in a layered distribution in the pebble center. This layered distribution is reflected in the radial packing factor, which exhibits an oscillatory decay, as shown in Fig. 7. In order to adapt to the cylindrical surface, a circular ring is formed by the pebble center of the first layer of pebbles in direct contact with the cylindrical wall, which were located at 0.5d from the wall. It is reflected as the first maximum point of the radial packing factor distribution in Fig. 7 and the first red circle areas with high packing factor in the local packing factor distribution, as shown in Fig. 8. Similarly, the 2nd, 3rd, and 4th maximum points of the radial packing factor and the 2nd, 3rd, and 4th circles formed by a high local packing factor correspond to the 2nd, 3rd, and 4th circles composed of pebble centers. In the central bulk zone of the pebble bed, pebbles are randomly and uniformly stacked, and the packing factor gradually tends to stable value. The phenomenon of radial packing factor oscillation only occurring within the range of 5d near the container wall is a major feature of the wall effect in random packed pebble beds with fixed walls.

The results of the radial packing factor calculated by line-based averaging method are compared with that of the arc-length based method proposed by Mueller [24], as shown in Fig. 7a. There is almost exact agreement between the different sets of results based on the line-based averaging method and the arc-length based method. The difference between the results of the current line-based averaging method and the arc-length based method shows a maximum difference of −0.9275 %. In addition, the results of radial packing factor of DEM simulation were also compared with that predicted by empirical model based on the experiment, as shown in Fig. 7b. It can be observed that the results are also agreement well. The difference they still get good consistency between them. The differences may be due to simplifications in discrete element simulations and material parameters that are different from experiments.

In addition, the local packing factor distributions in the cross-sectional plane and angular-radial plane were also calculated and figured, as shown in Fig. 8. The packing factor inside the pebble bed is shown in a more visual way. Local packing factor variations in the pebble bed due to wall effects are shown more clearly. In further, the local packing factor distributions in angular-radial plane of cylindrical

Table 1

Intersecting line segments and l_i (x, y, z_{low}, z_{up}) between pebble i and grid line (x, y).

Cases	Pebble height	Interaction type	l_i (x, y, z_{low}, z_{up})
1	$z_i > z_{up}$		$l_i(x,y,z_{low},z_{up}) = \sqrt{r_i^2 - L_{line}^2} - L_{pz}$ $= \sqrt{r_i^2 - \left[(x-x_i)^2 + (y-y_i)^2\right]} - \lvert z_i - z_{up}\rvert$
2	$z_{up} - r_i < z_i \leq z_{up}$		$l_i(x,y,z_{low},z_{up}) = \sqrt{r_i^2 - L_{line}^2} + L_{pz}$ $= \sqrt{r_i^2 - \left[(x-x_i)^2 + (y-y_i)^2\right]} + \lvert z_i - z_{up}\rvert$
3	$z_{low} + r_i < z_i \leq z_{up} - r_i$		$l_i(x,y,z_{low},z_{up}) = 2\sqrt{r_i^2 - L_{line}^2}$ $= 2\sqrt{r_i^2 - \left[(x-x_i)^2 + (y-y_i)^2\right]}$
4	$z_{low} < z_i \leq z_{low} + r_i$		$l_i(x,y,z_{low},z_{up}) = \sqrt{r_i^2 - L_{line}^2} + L_{pz}$ $= \sqrt{r_i^2 - \left[(x-x_i)^2 + (y-y_i)^2\right]} + \lvert z_i - z_{low}\rvert$
5	$z_{low} - r_i < z_i \leq z_{low}$		$l_i(x,y,z_{low},z_{up}) = \sqrt{r_i^2 - L_{line}^2} - L_{pz}$ $= \sqrt{r_i^2 - \left[(x-x_i)^2 + (y-y_i)^2\right]} - \lvert z_i - z_{low}\rvert$

pebble bed was revealed for the first time, as shown in Fig. 8b. The ability to calculate and plot contour maps of local packing factor distributions for columnar pebble beds of arbitrary shapes is the main feature of the line-averaging method proposed in this work.

5. Application in annular and other shaped pebble bed

5.1. Packing factor in annular pebble bed

In various applications of pebble beds, the fuel pebbles of high-temperature gas-cooled reactors (HTGR) accumulate in the reactor core into an annular pebble bed [33,34], while the tritium breeder pebbles in a water-cooled ceramic breeder (WCCB) blanket of fusion reactors are packed into an annular tube [35]. Therefore, the annular
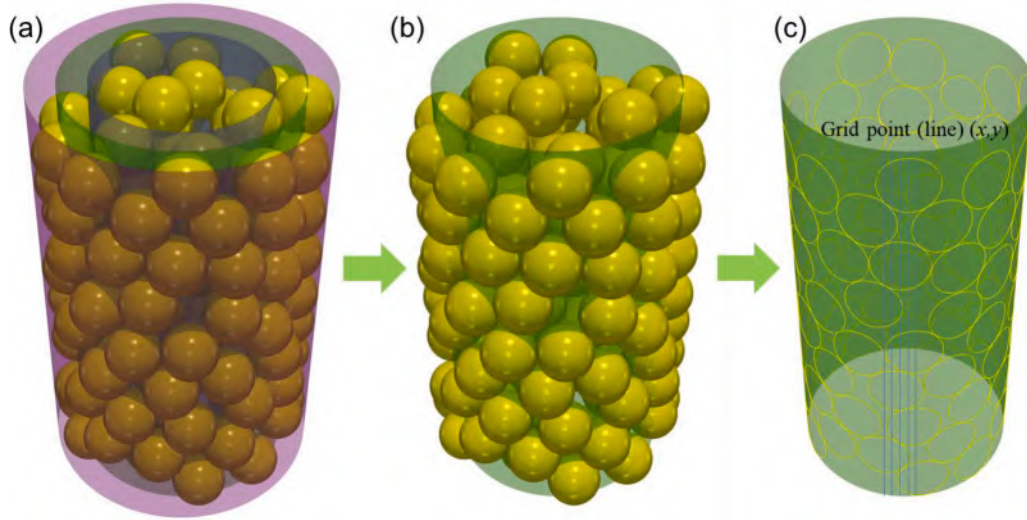
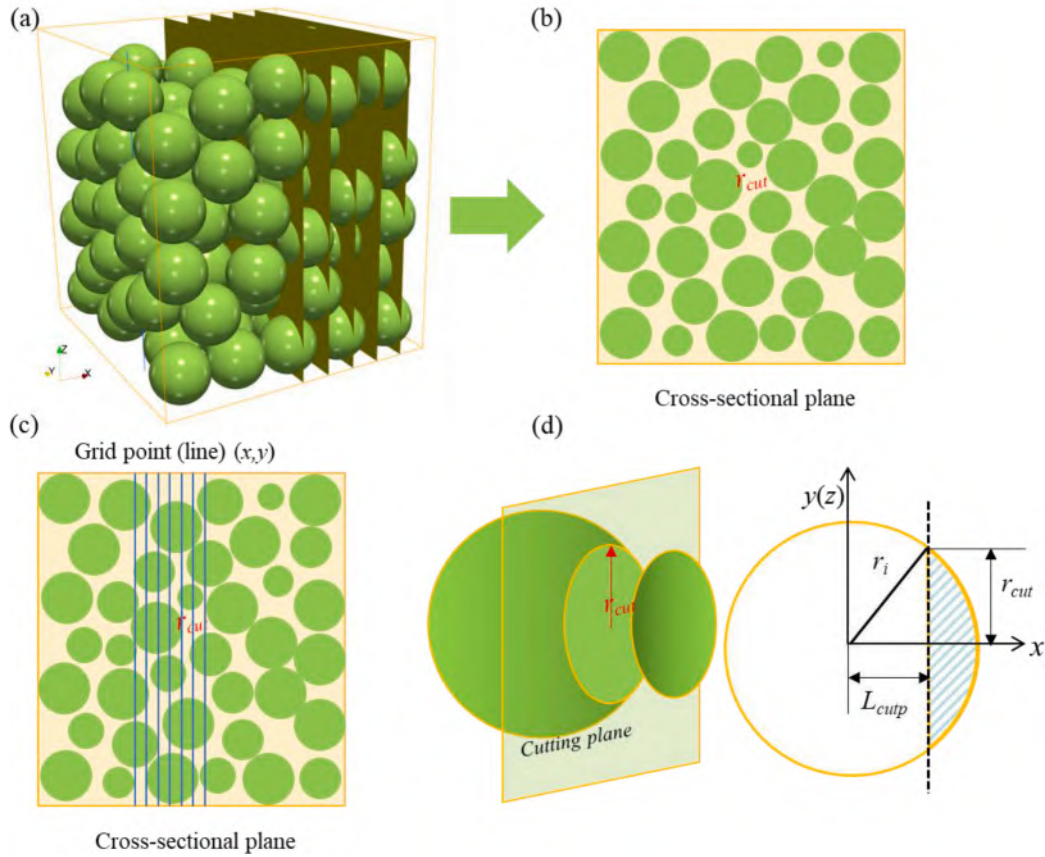**Fig. 4.** Calculation method of radial packing factor in pebble beds.

Fig. 5. Calculation method of axial packing factor in pebble beds [26]: (a) pebble bed, (b)cutting plane, (c) grid line in cutting plane, (d) calculation of cross-sectional circle area.

pebble bed packing structures were also analyzed by the line-averaged method. Fig. 9 shows the two annular pebble beds with same inner diameter Di = 5 mm, pebble diameter d = 1 mm, widths of these two annular are 10 mm and 15 mm respectively. The radial packing factor and local packing factor distribution are also calculated based on the line-based averaging method and plotted in Figs. 10 and 11.

Fig. 10 shows the radial packing factor variation with the distance to the inner side cylindrical walls, which can reflect the pebbles packing structures near convex and concave cylindrical surfaces. Fig. 10a shows

that although the radial packing factor exhibits an oscillation and damping characteristic as the distance to the wall increases, the oscillation region close to the concave and convex cylindrical surfaces is different from that close to a flat plane. When D_i = 5d, after the oscillation about 3d close to the inner convex cylindrical surface, the radial packing factor gradually tends to a stable value. However, near the outer concave cylindrical wall, the radial packing factor still oscillates within the range of 5d close to the concave wall. When the width of the annular channel increases to 15d, the oscillation region of the radial packing
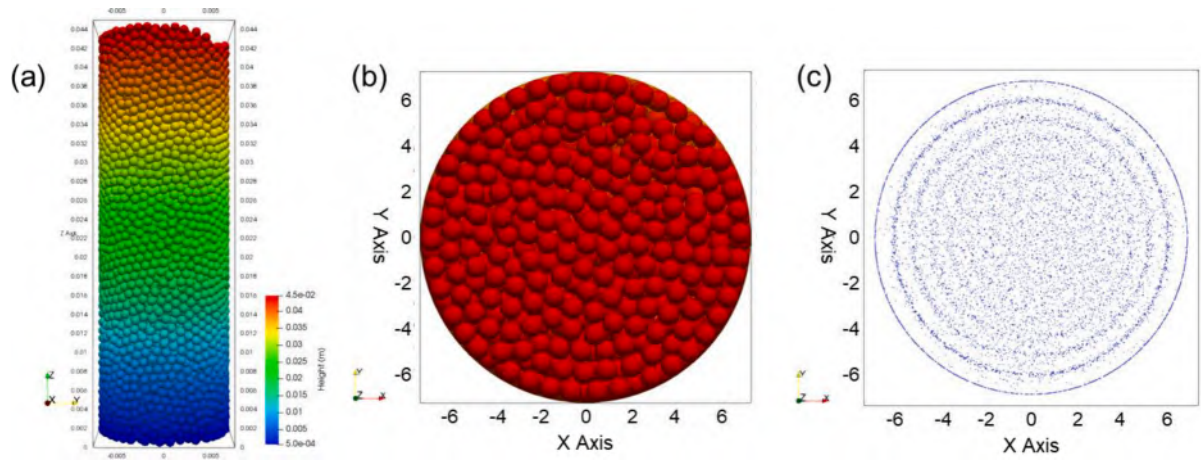
Fig. 6. Cylindrical beds packed with mono-sized pebbles: a) pebble bed; b) top view; c) pebble center distribution.
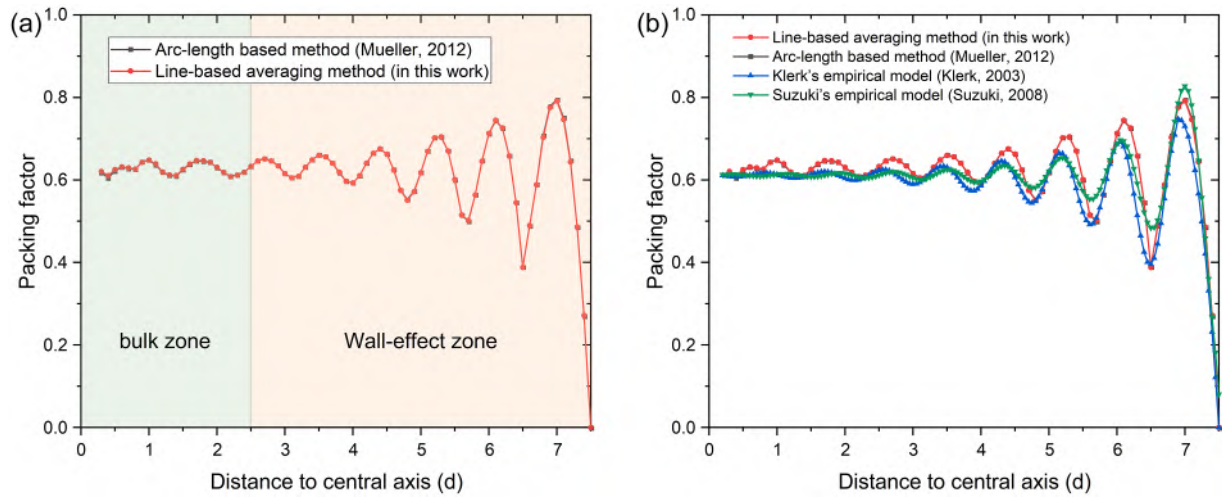

Fig. 7. Radical packing factor distribution in cylindrical beds based on the line-based averaging method: a) comparison with arc-length based method; b) comparison with empirical model.
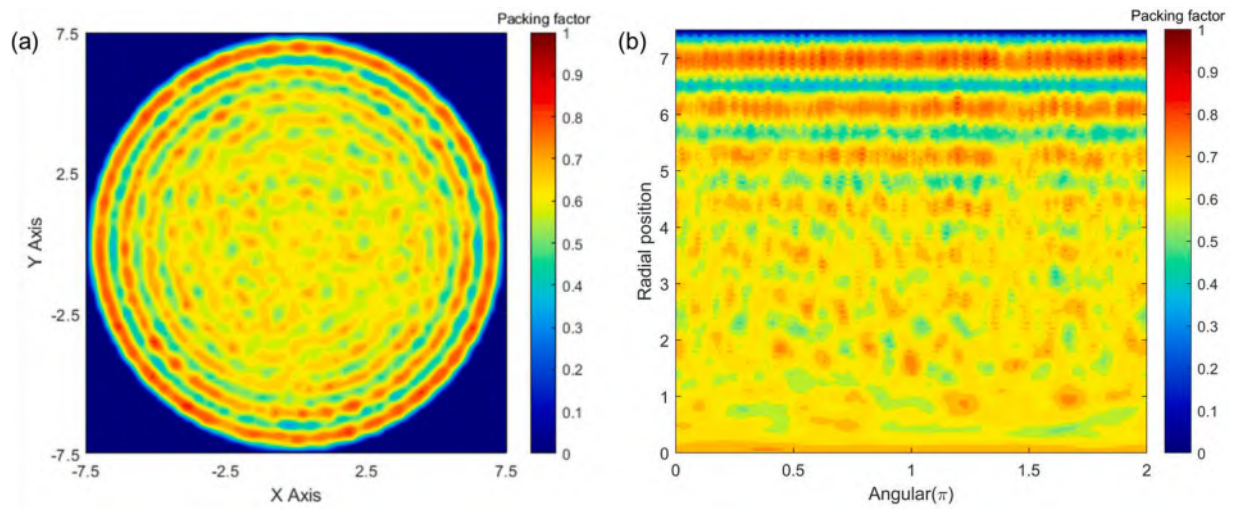

Fig. 8. Local packing factor distribution of cylindrical beds packed with mono-sized pebbles: a) cross-sectional distribution; b) angularly distribution.
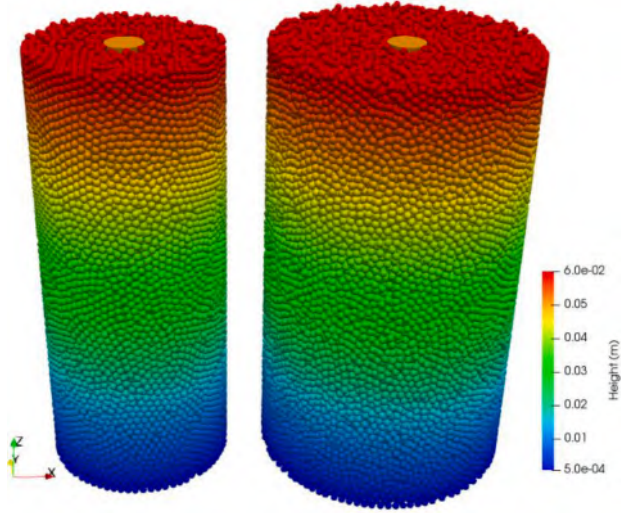
Fig. 9. Annular pebble beds with a) *di* = 5d, *w* = 10d; b) *di* = 5d, *w* = 15d.

the middle of the pebble bed. The oscillation characteristics of the packing factor near the convex cylindrical wall are related to Di/d, which will be conduct in the future, not in this paper.

Fig. 11 shows the local packing factor distribution in annular pebble beds. The wall effect of the local packing factor distribution can be clearly observed. Compared to cylindrical pebble beds, due to the presence of a central column inside the annular pebble bed, wall effects are also observed near the internal cylindrical surface. Compared to the concave cylindrical surface on the outside, the number of the rings with high packing factor near the inner convex cylindrical surface is reduced, which is consistent with the changes in radial packing factor distribution in Fig. 10.

For annular pebble beds, the packing factor of the bed is affected by both the width and the inner diameter (or outer diameter of cylindrical wall). There is a significant difference of the radial and local packing factor distribution of annular pebble bed between pebbles close to the inner convex cylindrical wall and close to the outer concave cylindrical wall, which needs to be studied more thoroughly, especially with smaller diameters ratio pebble beds.

5.2. Packing factor in other shaped pebble beds

The ability to calculate and plot contour maps of local packing factor distributions for arbitrary shaped columnar packed pebble beds is the

factor near the inner cylindrical wall is still limited to the range of 3d, while it is limited to the range of 5d near the outer cylindrical wall. The radial packing factor reaches a stable value within a range of about 7d in
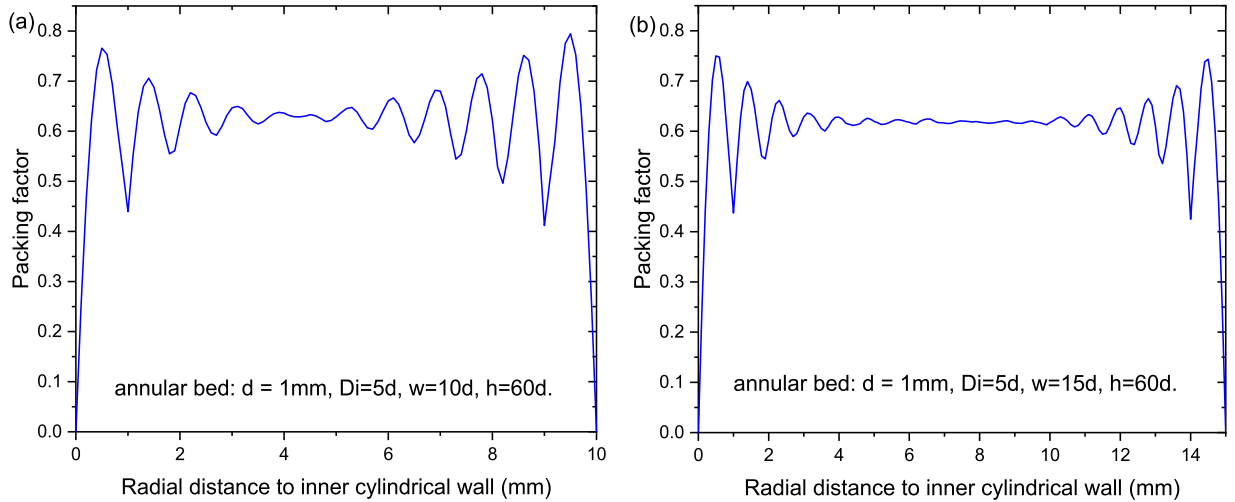

Fig. 10. Radial packing factor along the distance to inner cylindrical wall: a) *di* = 5d, *w* = 10d; b) *di* = 5d, *w* = 15d.
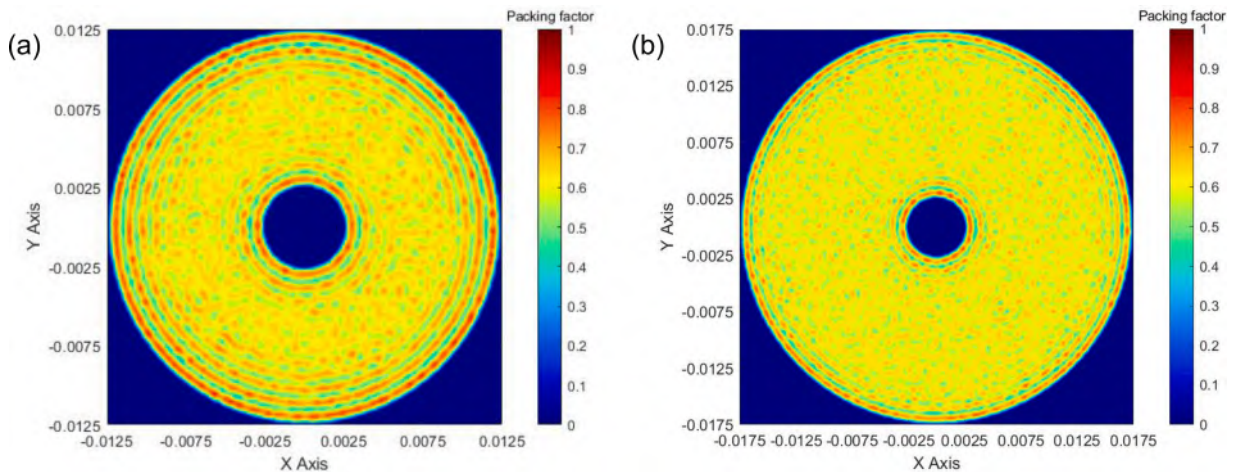

Fig. 11. Local packing factor distribution: a) *di* = 5d, *w* = 10d; b) *di* = 5d, *w* = 15d.

main feature of the line-averaging method proposed in this work, such as, annular, U-shaped and other shaped pebble beds.

For example, in some other special applications, pebbles are not stacked in cylindrical or square containers, but filled in other special irregular shaped containers, such as in the helium cooled ceramic breeder (HCCB) blanket of fusion reactors [36,37], where tritium breeders are stacked in the U-shaped cavity. Hence, in this section, the pebbles packing in U-shaped and hexagonal containers were analyzed by the line-based averaging method. Fig. 12 shows the mono-sized pebble packing in U-shaped and hexagonal container. In these two pebble beds, pebble diameter d is 2 mm. Pebble bed heights are 100 mm and 80 mm respectively.

Fig. 13 shows the local packing factor distribution of U-shaped pebble bed and hexagonal pebble bed, which are calculated using the line-averaged method, respectively. It can be seen that in the region near the wall of the pebble bed container, there is a layered distribution of high packing factors along the wall, and its variation characteristics follow the wall of the container. For example, in a U-shaped pebble bed, a U-shaped structure is also formed in the first layer of high packing factor area near the wall; Similarly, the high packing factor near the wall in a hexagonal pebble bed also forms a hexagonal shape; These high local packing factor regions are mainly contributed by pebbles in direct contact with the container wall; This is mainly because granular matter has fluid characteristics. During the packing process, the pebble flow can fill any other shaped container.

Particularly, the axial and radial packing factor distribution in different regions of the U-shaped pebble bed are also calculated, as shown in Fig. 14. The width of the pebble bed $w = 10d$. The diameter of the inner convex wall is 12.5d, the diameter of the outer concave wall is 32.5d. The entire U-shaped pebble bed was divided into 5 regions, as shown in Fig. 14a. Among them, Fig 11b represents the axial packing factor distribution in a rectangular area. The axial distribution characteristics of the packing factor in the arm region of the U-shaped pebble bed are similar to those of the rectangular pebble bed, and the packing factor presents a symmetrical distribution feature. However, in the bend region (as shown in region ④ and ⑤ in Fig. 14), it can be observed that the radial packing factor in this region has asymmetric distribution characteristics, similar to the distribution characteristics of a annular pebble bed. When approaching the convex surface on the inner side, the oscillation region of the radial packing factor is relatively small, which is mainly because this area can be considered as a 1/4 annular pebble bed. Thus the pebble packing close to a convex cylinder wall will be

investigated in future.

6. Conclusion

Local packing factor distribution can reveal the local structural features of random pebble packing, which have a great influence on the heat and mass transfer behaviors and mechanical properties of a pebble packed bed. Thus, in this work, a line-based averaging method was proposed to calculation the local packing factor or local porosity distribution. This method was extended and improved upon the development of Feng [26]. The validation was implemented by comparing the results with those obtained from experimental and numerical studies of cylindrical packed pebble bed. There is almost exact agreement between the different sets of results based on the line-based averaging method and the arc-length based method. The local packing factor distributions in angular-radial plane of cylindrical pebble bed was revealed for the first time. In further, the line-based averaging method have been applied to reveal the local packing factor distribution in the annular pebble beds, U-shaped pebble beds and hexagonal pebble beds.

This method can be applied to evaluate radial packing factor, axial packing factor and local packing factor by selecting a specific region to average, especially for the irregular shaped pebble beds. The ability to calculate and plot contour maps of local packing factor or porosity distributions for columnar pebble beds of arbitrary shapes is the main feature of the line-based averaging method, especially the local packing factor distributions in the cross-sectional plane and angular-radial plane.

CRediT authorship contribution statement

Baoping Gong: Writing – review & editing, Writing – original draft, Visualization, Validation, Methodology, Investigation, Funding acquisition, Formal analysis, Conceptualization. **Hao Cheng:** Writing – review & editing, Methodology, Investigation, Formal analysis, Conceptualization. **Juemin Yan:** Writing – review & editing, Methodology, Conceptualization. **Long Zhang:** Writing – review & editing, Resources, Project administration, Methodology.

Declaration of competing interest

The authors declare that they have no known competing financial interests or personal relationships that could have appeared to influence the work reported in this paper.
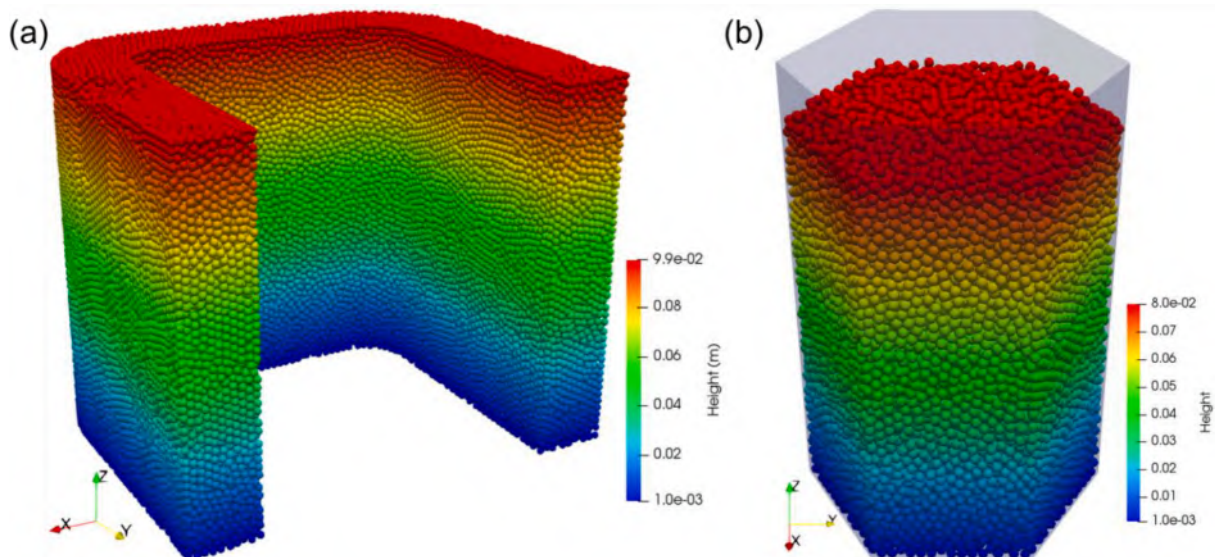

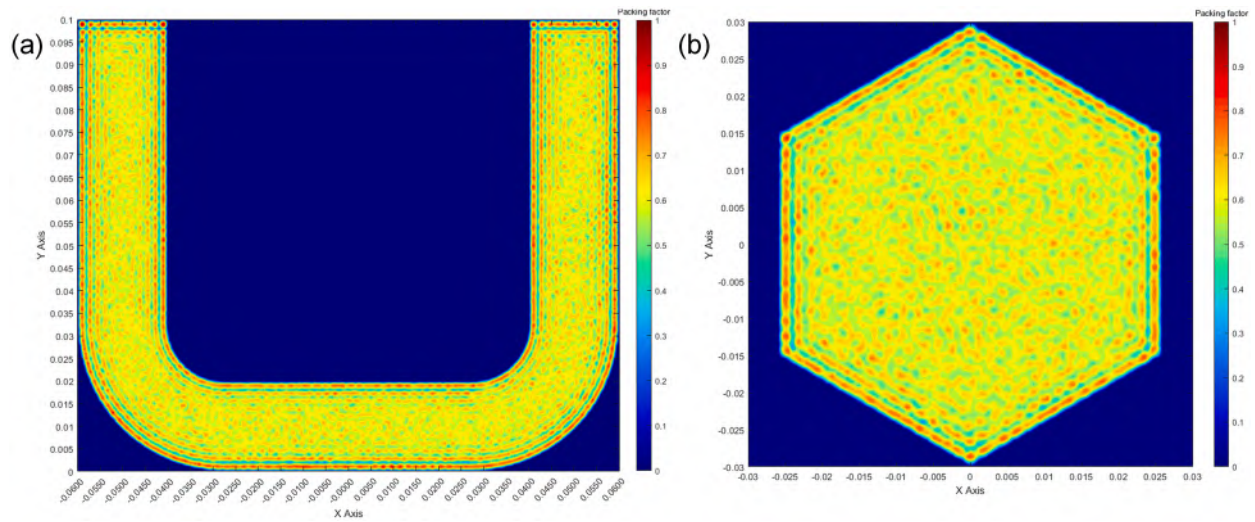**Fig. 12.** Pebbles packing in the a) U-shaped container and b) hexagonal container.

Fig. 13. Pebbles packing in the a) U-shaped container and b) hexagonal container.
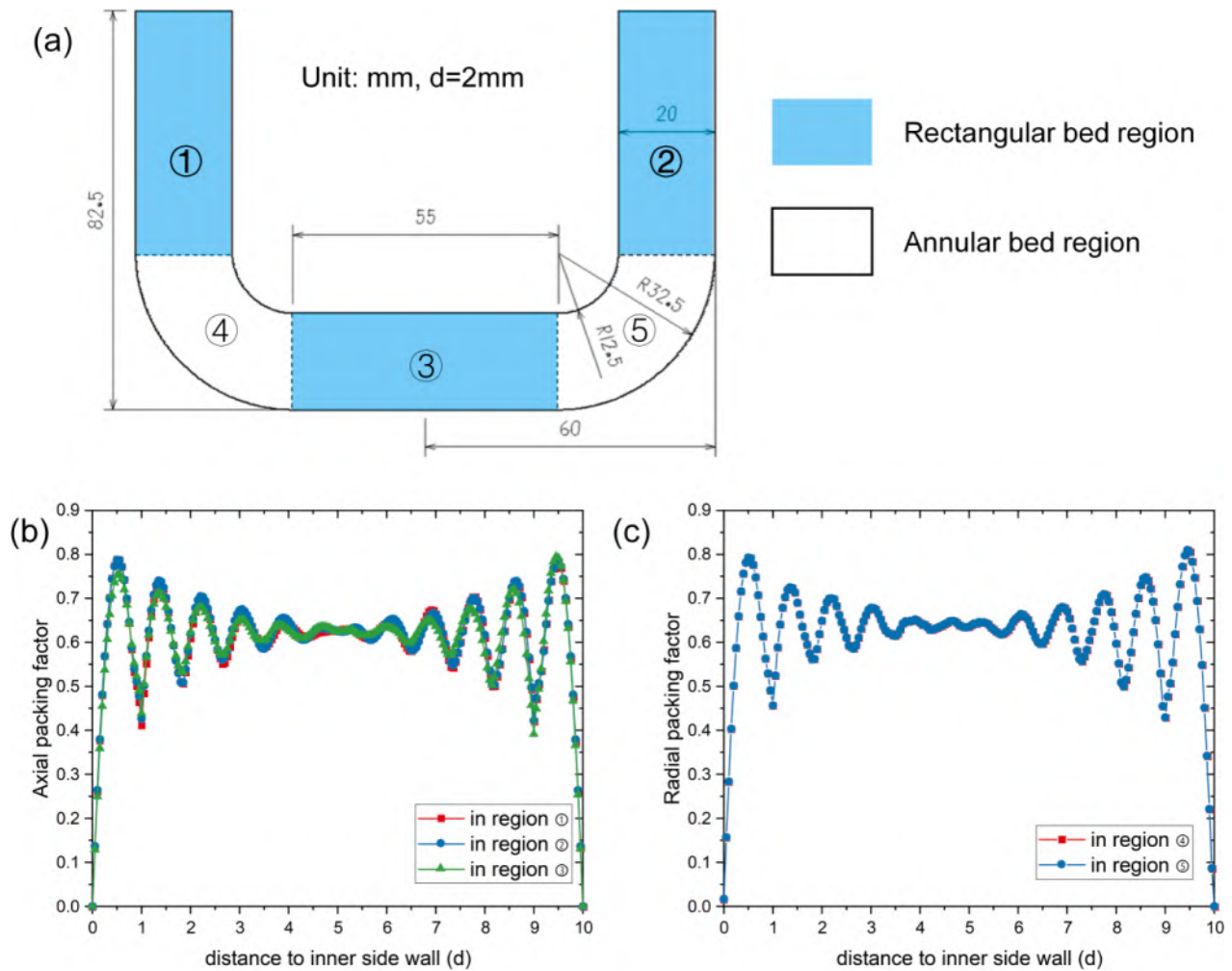

Fig. 14. Radial/axial packing factor distribution in the U-shaped pebble beds.

Data availability

Data will be made available on request.

Acknowledgments

References

[1] D. Mandal, D. Sathiyamoorthy, M. Vinjamur, Void fraction and effective thermal conductivity of binary particulate bed, Fusion Eng. Des. 88 (2013) 216–225.

[2] D.-O. Kim, S.-P. Hwang, D. Sohn, DEM study of packing and connectivity of binary-sized pebbles according to their size and mixing ratios under vibration conditions, Fusion Eng. Des. 168 (2021) 112648.

[3] Y. Gan, M. Kamlah, Discrete element modelling of pebble beds: with application to uniaxial compression tests of ceramic breeder pebble beds, J. Mech. Phys. Solids. 58 (2010) 129–144.

[4] D. Mandal, S. Gupta, Effective thermal conductivity of unary particulate bed, Can. J. Chem. Eng. 94 (2016) 1918–1923.

[5] B. Hu, B. Zhou, S. Bu, et al., Holistic hydraulic simulation for pebble bed using porous media approach, Energies 17 (2024) 3562.

[6] D. Mandal, M. Vinjamur, D. Sathiyamoorthy, Hydrodynamics of beds of small particles in the voids of coarse particles, Powder Technol. 235 (2013) 256–262.

[7] Y. Feng, K. Feng, Y. Liu, et al., Experimental investigation of thermal properties of the Li$_4$SiO$_4$ pebble beds, J. Plasma Fusion Re. Ser. 11 (2015) 49–52.

[8] B. Gong, Y. Feng, G. Yu, et al., Experimental investigation of the effect of particle size on the effective thermal properties of particle beds, J. Eng. Thermophys. 40 (2019) 1151–1159.

[9] B. Gong, H. Cheng, J. Yan, et al., Effects of the aspect ratio and cross-sectional area of rectangular tubes on packing characteristics of mono-sized pebble beds, Energies 16 (2023) 570.

[10] Z. Wu, Y. Wu, S. Tang, et al., DEM-CFD simulation of helium flow characteristics in randomly packed bed for fusion reactors, Prog. Nucl. Energy 109 (2018) 29–37.

[11] D. Choi, S. Park, J. Han, et al., A DEM-CFD study of the effects of size distributions and packing fractions of pebbles on purge gas flow through pebble beds, Fusion Eng. Des. 143 (2019) 24–34.

[12] B. Gong, H. Cheng, B. Zhou, et al., Investigation of wall effect on packing structures and purge gas flow characteristics in pebble beds for fusion blanket by combining discrete element method and computational fluid dynamics simulation, Appl. Sci. 14 (2024) 2289.

[13] Z. Li, K. Feng, Z. Zhao, et al., Neutronics study on HCCB blanket for CFETR, in: Fusion Eng. Des., 124, 2017, pp. 1273–1276.

[14] R.K. Annabattula, Y. Gan, S. Zhao, et al., Mechanics of a crushable pebble assembly using discrete element method, J. Nucl. Mater. 430 (2012) 90–95.

[15] H. Wu, N. Gui, X. Yang, et al., A smoothed void fraction method for CFD-DEM simulation of packed pebble beds with particle thermal radiation, Int. J. Heat. Mass Transf. 118 (2018) 275–288.

[16] N. Gui, S. Jiang, X. Yang, et al., A review of recent study on the characteristics and applications of pebble flows in nuclear engineering, Exp. Comput. Multiph. Flow. 4 (2022) 339–349.

[17] J. Reimann, J. Vicente, E. Brun, et al., X-ray tomography investigations of mono-sized sphere packing structures in cylindrical containers, Powder Technol. 318 (2017) 471–483.

[18] N. Romijn, Y.E.I. Bergmans, V. de Haas, et al., Reconstruction of particle positions and orientations from 3D MRI images of non-spherical particle packings, Particuology (2023).

[19] D. Mandal, V.K. Sharma, H.J. Pant, et al., Quality of fluidization in gas–solid unary and packed fluidized beds: an experimental study using gamma ray transmission technique, Powder Technol. 226 (2012) 91–98.

[20] Y. Gan, M. Kamlah, J. Reimann, Computer simulation of packing structure in pebble beds, Fusion Eng. Des. 85 (2010) 1782–1787.

[21] G.E. Mueller, Radial void fraction distributions in randomly packed fixed beds of uniformly sized spheres in cylindrical containers, Powder Technol. 72 (1992) 269–275.

[22] J. Theuerkauf, P. Witt, D. Schwesig, Analysis of particle porosity distribution in fixed beds using the discrete element method, Powder Technol. 165 (2006) 92–99.

[23] G.E. Mueller, Radial porosity in packed beds of spheres, Powder Technol. 203 (2010) 626–633.

[24] G.E. Mueller, A simple method for determining sphere packed bed radial porosity, Powder Technol. 229 (2012) 90–96.

[25] P.M. Bester, C.G. du Toit, A methodology to analyse the angular, radial and regional porosities of a cylindrical packed bed of spheres, Nucl. Eng. Des. 392 (2022) 111766.

[26] Y. Feng, B. Gong, H. Cheng, et al., Effects of bed dimension, friction coefficient and pebble size distribution on the packing structures of the pebble bed for solid tritium breeder blanket, Fusion Eng. Des. 163 (2021) 112156.

[27] L. Chen, Y. Chen, K. Huang, et al., Investigation of the packing structure of pebble beds by DEM for CFETR WCCB, J. Nucl. Sci. Technol. 53 (2016) 803–808.

[28] C.G. Du Toit, Evaluation of Approximate expressions to calculate the area of the intersection between a sphere and a cylindrical plane, Powders 1 (2022) 243–261.

[29] F.S. Mederos, J. Ancheyta, J. Chen, Review on criteria to ensure ideal behaviors in trickle-bed reactors, Appl. Catal. A 355 (2009) 1–19.

[30] S. Jiang, J. Tu, X. Yang, et al., A review of pebble flow study for pebble bed high temperature gas-cooled reactor, Exp. Comput. Multiph. Flow. 1 (2019) 159–176.

[31] A. de Klerk, Voidage variation in packed beds at small column to particle diameter ratio, AIChE J. 49 (2003) 2022–2029.

[32] M. Suzuki, T. Shinmura, K. Iimura, et al., Study of the wall effect on particle packing structure using X-ray micro computed tomography, Adv. Powder Technol. 19 (2008) 183–195.

[33] C. Ren, X.-T. Yang, Y.-F. Sun, Porous structure analysis of the packed beds in a high-temperature reactor pebble bed modules heat transfer test facility, Chin. Phys. Lett. 30 (2013) 022801.

[34] C.G. Du Toit, Radial variation in porosity in annular packed beds, Nucl. Eng. Des. 238 (2008) 3073–3079.

[35] M. Lei, S. Xu, C. Guo, et al., Design and thermal-hydraulic evaluation of helium-cooled ceramic breeder blanket for China fusion engineering test reactor, Int. J. Energy Res. 42 (2018) 1657–1663.

[36] X.Y. Wang, K.M. Feng, Y.J. Chen, et al., Current design and R&D progress of the Chinese helium cooled ceramic breeder test blanket system, Nucl. Fusion 59 (2019) 076019.

[37] B. Gong, Y. Feng, H. Liao, et al., Numerical investigation of the pebble bed structures for HCCB TBM, Fusion Eng. Des. 136 (2018) 1444–1451.